



# Cross-Species Translation of Biophase Half-Life and Potency of GalNAc-Conjugated siRNAs

Alessandro Boianelli,<sup>1</sup> Yasunori Aoki,<sup>1</sup> Maxim Ivanov,<sup>2</sup> Anders Dahlén,<sup>3</sup> and Peter Gennemark<sup>1,4</sup>

Small interfering RNAs (siRNAs) with *N*-acetylgalactosamine (GalNAc) conjugation for improved liver uptake represent an emerging class of drugs to treat liver diseases. Understanding how pharmacokinetics and pharmacodynamics translate is pivotal for *in vivo* study design and human dose prediction. However, the literature is sparse on translational data for this modality, and pharmacokinetics in the liver is seldom measured. To overcome these difficulties, we collected time-course biomarker data for 11 GalNAc–siRNAs in various species and applied the kinetic-pharmacodynamic modeling approach to estimate the biophase (liver) half-life and the potency. Our analysis indicates that the biophase half-life is 0.6–3 weeks in mouse, 1–8 weeks in monkey, and 1.5–14 weeks in human. For individual siRNAs, the biophase half-life is 1–8 times longer in human than in mouse, and generally 1–3 times longer in human than in monkey. The analysis indicates that the siRNAs are more potent in human than in mouse and monkey.

**Keywords:** GalNAc-conjugated siRNA, KPD modeling, biophase half-life, translation

## Introduction

**N**-ACETYLGALACTOSAMINE (GalNAc)-conjugated small interfering RNAs (siRNAs) are double-stranded molecules containing a sense and an antisense strand, of which the latter elicits the pharmacological effect [1]. These drugs are designed to knock down a certain gene with complementary nucleotide sequences by degrading mRNA after transcription, and as an effect preventing translation. The GalNAc conjugation targets the siRNA specifically to the liver, and GalNAc–siRNAs represent an emerging class of drugs to treat various liver diseases [2].

Understanding how pharmacokinetics and pharmacodynamics translate between species is pivotal to set dose level and dosing schedule in preclinical proof-of-concept studies, to predict the human dose from preclinical data, and to set safety margins. Important translational data in this direction were recently reported in Ref. [3]. However, the literature is generally sparse on translational data for these GalNAc–siRNAs, and pharmacokinetics in the liver is seldom measured.

One way to learn more about translation of GalNAc–siRNAs is to estimate drug pharmacokinetics in the liver, target turnover, and siRNA potency from temporal biomarker data using mathematical dose–response modeling, so-called kinetic-pharmacodynamic (KPD) modeling [4]. Previous study in this direction on oligonucleotides mainly considered antisense oligonucleotides and human data [5]. In this study, we present an analysis of 11 GalNAc–siRNAs in several species. Specifically, we estimate biophase (liver) half-life and potency across species of GalNAc–siRNAs that have reached the clinical phase and for which data are available.

## Materials and Methods

We collected and digitized available literature time-course biomarker data from mice, monkeys (rhesus macaque *Macaca mulatta* or cynomolgus *Macaca fascicularis*), and humans of the following 11 GalNAc–siRNAs: Revusiran [6–8], Vutrisiran [9], Cemdisiran [10,11], Givlaari (Givosiran) [12,13], Lumasiran [14,15], Fitusiran [16,17], Inclisiran

<sup>1</sup>Drug Metabolism and Pharmacokinetics, Research and Early Development, Cardiovascular, Renal and Metabolism (CVRM), BioPharmaceuticals R&D, AstraZeneca, Gothenburg, Sweden.

<sup>2</sup>Quantitative Biology SE, Data Sciences and Quantitative Biology, Discovery Sciences, AstraZeneca, Gothenburg, Sweden.

<sup>3</sup>Oligonucleotide Discovery, Discovery Sciences, BioPharmaceuticals R&D, AstraZeneca, Gothenburg, Sweden.

<sup>4</sup>Department of Biomedical Engineering, Linköping University, Linköping, Sweden.

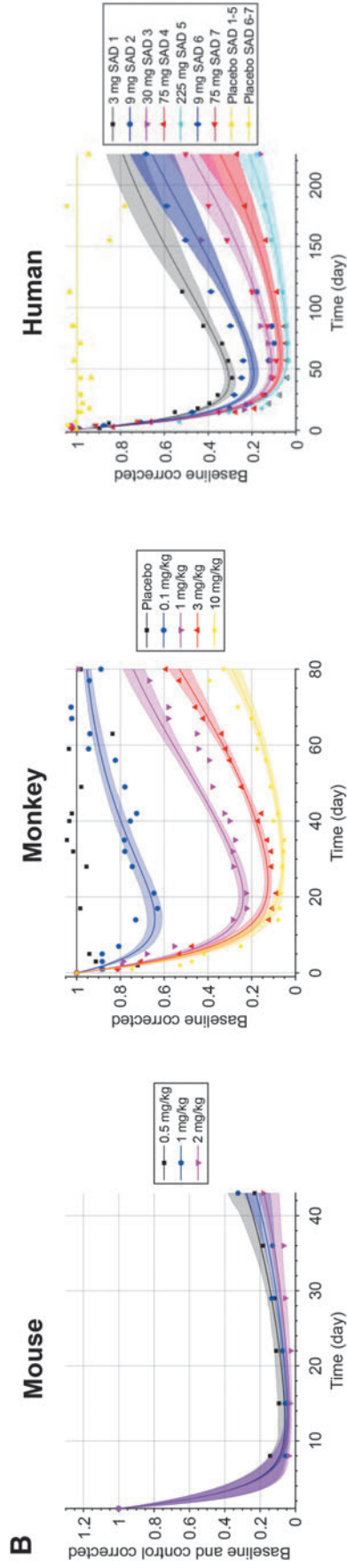
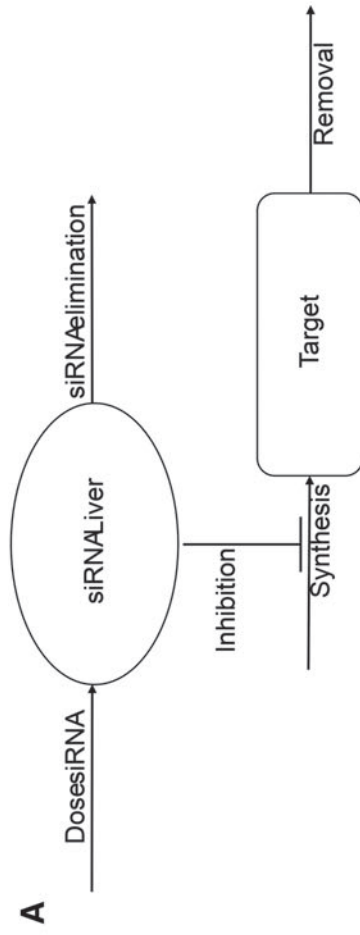


**FIG. 1.** (A) Schematic diagram of the K-PD model. The amount of siRNA in the liver is governed by the dose and elimination rate. This amount inhibits the synthesis rate of the target according to the mode of action of siRNAs. Target is eliminated by its natural half-life. (B) Example of K-PD model fits to data for mouse, monkey, and human for different dose levels of Olpasiran. K-PD, kinetic-pharmacodynamic; siRNAs, small interfering RNAs.



[18–20], ALN-HBV02 [21,22], ARO-APOC3 [23–26], ARO-ANG3 [27–30], and Olpasiran [31]. Compounds for which we could at least find relevant human data were included in the analysis. Group mean data were digitized using MATLAB (R2020a; The MathWorks, Natick, MA) or WebplotDigitizer (Ver. 4.5; Automeris, Pacifica, CA).

We applied the K-PD modeling approach to estimate the biophase half-life in the target organ and the potency ( $IDK_{50}$ , ie, the dose per unit of time that results in 50% reduction in the target mRNA or protein), see Fig. 1. The pharmacokinetics is described by a virtual one-compartment model aimed to represent the biophase. No drug concentration measurements are required, or available, and the model depends solely on the biomarker data for identification of all parameters. We used an indirect-response PD model, where the drug inhibits the zero-order synthesis rate  $k_{in}$  of response.

In the model, the synthesis rate constant  $k_S$  of response ( $R$ ) is inhibited by a virtual infusion rate ( $IR$ ), expressed in drug amount ( $A$ ) per time unit, through a sigmoid Emax model:

$$dA(t)/dt = -k_{elim} \times A(t) \quad (1)$$

$$IR(t) = A(t) \times k_{elim} \quad (2)$$

$$k_S(t) = k_{in} \times \left(1 - IR(t)^\gamma / (IDK_{50}^\gamma + IR(t)^\gamma)\right) \quad (3)$$

$$dR(t)/dt = k_S(t) - R(t) \times k_{out} \quad (4)$$

$$R(0) = k_{in}/k_{out}, A(0) = Dose, \quad (5)$$

where  $k_{elim}$  represents the elimination rate constant from the virtual compartment,  $k_S$  and  $k_{out}$  are the zero-order synthesis and the first-order degradation rate constants of the response  $R$ ,  $R(0)$  is the baseline value of the response,  $k_S$  is the time-dependent synthesis rate constant,  $IDK_{50}$  represents  $IR$  that leads to 50% inhibition of  $k_S$ ,  $IDK_{50}$  represents the apparent *in vivo* potency of the drug reflecting the ratio of clearance and bioavailability as well as the intrinsic potency of the drug, and  $\gamma$  is the Hill coefficient.

Numerical analyses were performed in MATLAB (R2020a; The MathWorks, Natick, MA). Specifically, the Matlab

function *fminsearch* was used for solving the optimization problems encountered during parameter estimation. Parameter estimation was performed according to a maximum likelihood approach with an additive error model, using the naive-pooled data approach.

## Results and Discussion

Mouse, monkey, and human data were collected and digitized for 7, 8, and 11 of the considered GalNAc-conjugated siRNAs, respectively. Model parameters were generally well estimated in terms of confidence intervals (Table 1 and Supplementary Information). For example, Fig. 1B shows the data and model fit for Olpasiran. The analysis indicates that the biophase half-life of GalNAc-conjugated siRNAs is 0.6–3 weeks in mice, 1–8 weeks in monkey, and 1.5–14 weeks in humans.

For individual siRNAs, the biophase half-life is 1–8 times longer in human than in mouse, and generally 1–3 times longer in human than in monkey (Fig. 2A). Givlaari deviates from the general pattern with a 28 times longer biophase half-life in human than in monkey. There is no clear dependency between translation of half-life between species and type of chemistry (indicated by the colors of the markers in Fig. 2A).

Potencies in form of  $IDK_{50}$  were relatively similar between mice and monkeys, and greater in humans. Specifically,  $IDK_{50}$  was predicted to be similar or smaller (up to 30-fold) in human than in mouse, and similar or smaller (up to 100-fold) in human than in monkey (Fig. 2B). Similarly to half-life, there is no clear dependency between translation of potency between species and type of chemistry. The higher potency observed in human is likely a result of optimization against the human sequence in the screening phase.

For two estimated half-lives, we could compare the results with previously reported data. First, the predicted biophase half-life of Fitusiran in human of ~3 weeks compares well with the predicted liver half-life of 20 days in Ref. [32]. Second, the predicted biophase half-life of Givlaari in monkey of 1.8 days compares well with the predicted distributional half-life of 2.1 days from a two-compartment model fit to measured liver concentration data by Ref. [33].

The approach taken is limited by the lack of publicly available biomarker data in some species for certain siRNAs, and by the modeling on group mean data and not on individual data. The approach is supported by two comparisons with available reported data of biophase half-lives. The

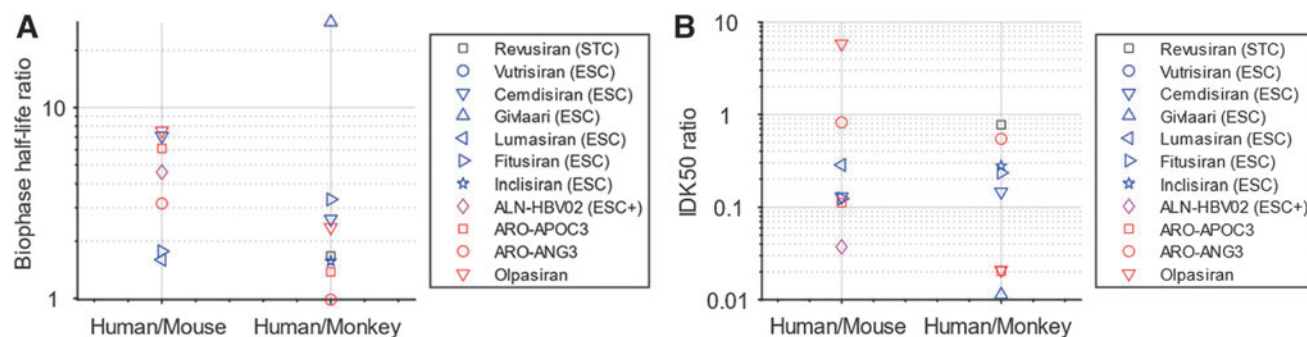


**FIG. 2.** Predicted ratios between human and mouse and between human and monkey for biophase half-life (A) and potency  $IDK_{50}$  (B) for the analyzed GalNAc-siRNAs. *Black*: Alnylam’s STC; *blue*: Alnylam’s ESC; *magenta*: Alnylam’s ESC-plus (ESC+); *red*: arrowhead Pharmaceuticals’ chemistry. Biophase half-life was calculated as  $\ln(2)/k_{elim}$ . ESC, enhanced stabilization chemistry; GalNAc, *N*-acetylgalactosamine; STC, standard template chemistry.

reported quantitative translational relationships may help guiding *in vivo* design and human dose predictions of GalNac-conjugated siRNAs. In conclusion, we present the first systematic translational investigation of biophase (liver) half-life and potency of GalNac-siRNAs.

#### Author Disclosure Statement

Authors are employed by AstraZeneca AB.

#### Funding Information

No external funding was received for this article.

#### Supplementary Material

Supplementary Data

#### References

- Crooke ST, BF Baker, RM Crooke and XH Liang. (2021). Antisense technology: an overview and prospectus. *Nat Rev Drug Discov* 20:427–453.
- Zhang MM, R Bahal, TP Rasmussen, JE Manautou and XB Zhong. (2021). The growth of siRNA-based therapeutics: updated clinical studies. *Biochem Pharmacol* 189:114432.
- Chong S, S Agarwal, S Agarwal, KC Aluri, M Arciprete, C Brown, K Charisse, J Cichocki, K Fitzgerald, *et al.* (2021). The nonclinical disposition and pk/pd properties of galnac-conjugated siRNA are highly predictable and build confidence in translation to man. *Drug Metab Dispos* 50:DMD-MR-2021-000428.
- Jacqmin P, E Snoeck, EA van Schaick, R Gieschke, P Pillai, JL Steimer and P Girard. (2007). Modelling response time profiles in the absence of drug concentrations: definition and performance evaluation of the k-pd model. *J Pharmacokinetic Pharmacodyn* 34:57–85.
- Jansson-Löfmark R and P Gennemark. (2018). Inferring half-lives at the effect site of oligonucleotide drugs. *Nucleic Acid Ther* 28:319–325.
- Butler JS, A Chan, S Costelha, S Fishman, JL Willoughby, TD Borland, S Milstein, DJ Foster, P Goncalves, *et al.* (2016). Preclinical evaluation of RNAi as a treatment for transthyretin-mediated amyloidosis. *Amyloid* 23:109–118.
- Rajeev K, T Zimmermann, M Manoharan, M Maier, S Kuchimanchi and K Charisse. (2014). RNAi agents, compositions and methods of use thereof for treating transthyretin (TTR) associated diseases. WO2015042564A1.
- Zimmermann TS, V Karsten, A Chan, J Chiesa, M Boyce, BR Bettencourt, R Hutabarat, S Nochur, A Vaishnav, *et al.* (2017). Clinical proof of concept for a novel hepatocyte-targeting galnac-siRNA conjugate. *Mol Ther* 25:71–78.
- Habtemariam BA, V Karsten, H Attarwala, V Goel, M Melch, VA Clausen, P Garg, AK Vaishnav, MT Sweetser, *et al.* (2021). Single-dose pharmacokinetics and pharmacodynamics of transthyretin targeting N-acetylgalactosamine-small interfering ribonucleic acid conjugate, vutrisiran, in healthy subjects. *Clin Pharmacol Ther* 109:372–382.
- Kusner LL, K Yucius, M Sengupta, AG Sprague, D Desai, T Nguyen, K Charisse, S Kuchimanchi, R Kallanthottathil, *et al.* (2019). Investigational RNAi therapeutic targeting c5 is efficacious in pre-clinical models of myasthenia gravis. *Mol Ther Methods Clin Dev* 13:484–492.
- Badri P, X Jiang, A Borodovsky, N Najafian, J Kim, VA Clausen, V Goel, B Habtemariam and G Robbie. (2021). Pharmacokinetic and pharmacodynamic properties of cemi-siran, an RNAi therapeutic targeting complement component 5, in healthy subjects and patients with paroxysmal nocturnal hemoglobinuria. *Clin Pharmacokinet* 60:365–378.
- EMA. (2020). Assessment report. Givosiran international non-proprietary name: Givosiran. EMEA/H/C/004775/0000.
- Sardh E, P Harper, M Balwani, P Stein, D Rees, DM Bissell, R Desnick, C Parker, J Phillips, *et al.* (2019). Phase 1 trial of an RNA interference therapy for acute intermittent porphyria. *N Engl J Med* 380:549–558.
- Erbe DV. (2020). Methods for inhibition of hao1 (hydroxyacid oxidase 1 (glycolate oxidase)) gene expression. WO2019014491A1.
- EMA. (2020). Assessment report oxlumo. EMA/568312/2020.
- Sehgal A, S Barros, L Ivanciu, B Cooley, J Qin, T Racie, J Hettinger, M Carioto, Y Jiang, *et al.* (2015). An RNAi therapeutic targeting antithrombin to rebalance the coagulation system and promote hemostasis in hemophilia. *Nat Med* 21:492–497.
- Pasi KJ, S Rangarajan, P Georgiev, T Mant, MD Creagh, T Lissitchkov, D Bevan, S Austin, CR Hay, *et al.* (2017). Targeting of antithrombin in hemophilia A or B with RNAi therapy. *N Engl J Med* 377:819–828.
- Borodovsky A, RG Kallanthottathil, K Fitzgerald, M Frank-Kamenetsky, W Querbes, M Maier, K Charisse, S Kuchimanchi, M Manoharan, *et al.* (2014). Pcsk9 siRNA compositions and methods of use thereof. WO2014089313A1.
- Borodovsky A, W Querbes, J Sutherland, R Hutabarat, S Milstein, S Kuchimanchi, R Kuchimanchi, K Charisse, K Yucius, *et al.* (2014). Development of monthly to quarterly subcutaneous administration of RNAi therapeutics targeting the metabolic diseases genes PCSK9, APOC3 and ANGPTL3. *Circulation* 130:A11936.
- Ray KK, U Landmesser, LA Leiter, D Kallend, R Dufour, M Karakas, T Hall, R Troquay, T Turner, *et al.* (2017). Inclisiran in patients at high cardiovascular risk with elevated LDL cholesterol. *N Engl J Med* 376:1430–1440.
- Gane E, Y-S Lim, D Cloutier, L Shen, A Cathcart, X Ding, P Pang, S Huang and R Yuen. Safety and antiviral activity of vir-2218, an X-targeting RNAi therapeutic, in participants with chronic hepatitis B infection: week 48 follow-up results. Available at: <https://investors.vir.bio/static-files/10c2cdad-2e8a-49c1-b8f7-a11d8906bc26> Accessed March 4, 2022.
- Stuart M, N Tuyen, A Castoreno, A Liebow, J Vasant, M Maier and L Sepp-Lorenzino. Preclinical development of an RNAi therapeutic drug candidate targeting hepatitis B virus, 2017. Available at: [https://www.alnylam.de/wp-content/uploads/2017/09/OTS-2017\\_Poster-4\\_Milstein-et-al..pdf](https://www.alnylam.de/wp-content/uploads/2017/09/OTS-2017_Poster-4_Milstein-et-al..pdf) Accessed January 27, 2022.
- Clifton P, D Sullivan, J Baker, C Schwabe, S Thackwray, R Scott, J Hamilton, T Chang, B Given, *et al.* (2020). Pharmacodynamic effect of aro-apoc3, an investigational hepatocyte-targeted RNA interference therapeutic targeting apolipoprotein c3, in patients with hypertriglyceridemia and multifactorial chylomicronemia. *Circulation* 142:A12594.
- Schwabe C, R Scott, DR Sullivan, J Baker, P Clifton, J Hamilton, B Given, S Melquist, J Knowles, *et al.* (2019). RNA interference targeting apolipoprotein c-III results in deep and prolonged reductions in plasma triglycerides. *Circulation* 140:E987.
- Schwabe C, R Scott, D Sullivan, J Baker, P Clifton, J Hamilton, B Given, J San Martin, S Melquist, *et al.* (2020). RNA interference targeting apolipoprotein c-III with aro-

- apoc3 in healthy volunteers mimics lipid and lipoprotein findings seen in subjects with inherited apolipoprotein c-iii deficiency. *Eur Heart J* 41:ehaa946.3330.
26. Li Z, Z Rui, T Pei, S Kanner and S Wong. (2019). Rna interference agents and compositions for inhibiting the expression of apolipoprotein c-iii (apoc3). WO2019051402A1.
  27. Watts GF, C Schwabe, R Scott, P Gladding, D Sullivan, J Baker, P Clifton, J Hamilton, B Given, *et al.* (2020). Pharmacodynamic effect of aro-ang3, an investigational rna interference targeting hepatic angiotensin-like protein 3, in patients with hypercholesterolemia. *Circulation* 142:A15751.
  28. Watts GF, C Schwabe, R Scott, P Gladding, DR Sullivan, J Baker, P Clifton, J Hamilton, B Given, *et al.* (2019). Rna interference targeting hepatic angiotensin-like protein 3 results in prolonged reductions in plasma triglycerides and ldl-c in human subjects. *Circulation* 140:E987–E988.
  29. Li Z, R Zhu and S Wong. (2019). Rnai agents and compositions for inhibiting expression of angiotensin-like 3 (angptl3), and methods of use. WO2019055633A1.
  30. Watts G, C Schwabe, R Scott, P Gladding, D Sullivan, J Baker, P Clifton, J Hamilton, B Given, *et al.* (2020). Rnai inhibition of angiotensin-like protein 3 (angptl3) with aro-ang3 mimics the lipid and lipoprotein profile of familial combined hypolipidemia. *Eur Heart J* 41:ehaa946.3331.
  31. Koren MJ, PM Moriarty, SJ Baum, J Neutel, M Hernandez-Illas, HS Weintraub, M Florio, H Kassahun, S Melquist, *et al.* (2022). Preclinical development and phase 1 trial of a novel sirna targeting lipoprotein(a). *Nat Med* 28:96–103.
  32. Attarwala H, V Goel, M Kate, A Akin and G Robbie. Development of a pharmacokinetic-pharmacodynamic (pk-pd) model of fitusiran, an investigational rna therapeutic targeting antithrombin for the treatment of hemophilia in patients with and without inhibitors. Available at: [https://www.alnylam.de/wp-content/uploads/2017/07/Attarwala\\_Fitusiran-PKPD\\_ISTH-2017\\_09July2017.pdf](https://www.alnylam.de/wp-content/uploads/2017/07/Attarwala_Fitusiran-PKPD_ISTH-2017_09July2017.pdf) Accessed January 27, 2022.
  33. Li J, J Liu, X Zhang, V Clausen, C Tran, M Arciprete, Q Wang, C Rocca, L-H Guan, *et al.* (2021). Nonclinical pharmacokinetics and absorption, distribution, metabolism, and excretion of givosiran, the first approved n-acetylgalactosamine-conjugated rna interference therapeutic. *Drug Metab Dispos* 49:572–580.

Address correspondence to:  
Alessandro Boianelli, PhD  
*Drug Metabolism and Pharmacokinetics,  
Research and Early Development  
Cardiovascular, Renal and Metabolism (CVRM)  
BioPharmaceuticals R&D  
AstraZeneca  
Gothenburg 43150  
Sweden*

*E-mail:* alessandro.boianelli@astrazeneca.com

Received for publication March 10, 2022; accepted after revision June 1, 2022.